Symposium: Applications of Inorganic Photochemistry

Modulation of the Photoluminescence of Semiconductors by Surface Adduct Formation: An Application of Inorganic Photochemistry to Chemical Sensing

Arthur B. Ellis,* Robert J. Brainard, Keith D. Kepler, Dale E. Moore, and Edmund J. Winder**
Department of Chemistry, University of Wisconsin–Madison, Madison, WI 53706

Thomas F. Kuech
Department of Chemical Engineering, University of Wisconsin–Madison, Madison, WI 53706

George C. Lisensky
Department of Chemistry, Beloit College, Beloit, WI 53511

Semiconductors provide a unique perspective on inorganic photochemistry. The electronic structure of common semiconductors permits a coupling of optical and electrical phenomena (*1*). As a consequence, semiconductors have found widespread use in many common electro-optical devices, including light-emitting diodes (LEDs), diode lasers, and solar cells. In the case of LEDs and diode lasers, electrical excitation produces a highly emissive excited state of the solid; in contrast, in solar cells, photoexcitation can produce an electrical output.

Interfaces derived from semiconducting solids afford opportunities for chemical control of their electro-optical properties. The intent of this article is to describe the construction and operation of chemical sensors based on the photoluminescence (PL) of semiconducting solids. We and others have shown that adduct formation involving the binding of ambient molecules to the semiconductor surface can lead to reversible PL changes that can be used as the basis for on-line sensor structures (*2, 3*). Because these devices link surface coordination chemistry to the electrical and excited-state properties of the semiconductor substrates, they provide a rich collection of applications of inorganic photochemistry.

Physical and Electronic Structure

Of the common inorganic semiconductors, the emissive II–VI compounds CdS and CdSe [CdS(e)] have proven to be particularly versatile sensor substrates. These solids have the wurtzite crystal structure, illustrated in Figure 1, which comprises hexagonal close-packed chalcogen atoms with half of the tetrahedral holes filled by cadmium atoms (*4*). Thus, each type of atom is tetrahedrally coordinated exclusively by atoms of the other type. Figure 1 also reveals the polar nature of the CdS(e) crystal: the (0001) face at the top of the figure consists exclusively of Cd atoms, and the opposing $(000\bar{1})$ face exclusively of chalcogen atoms (*5*). Most studies of adduct formation onto single-crystal CdS(e) samples have employed the more highly emissive (0001) face, which is more accurately described as a Cd-rich

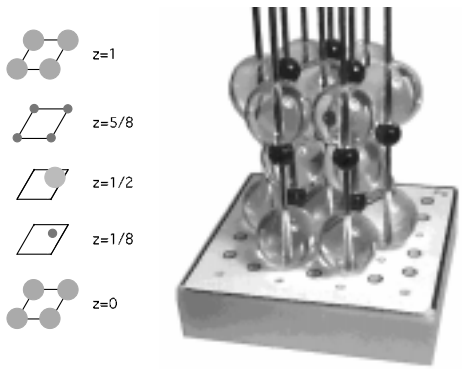

Figure 1. A model of the wurtzite crystal structure of CdS(e), constructed with the ICE Solid-State Model Kit. Large and small spheres represent chalcogen and cadmium atoms, respectively. A layer sequence for the unit cell of the wurtzite structure is shown alongside the model; centers of circles represent the location of the centers of atoms at the indicated altitude (*z*-value) from the base of the unit cell ($z = 0$).

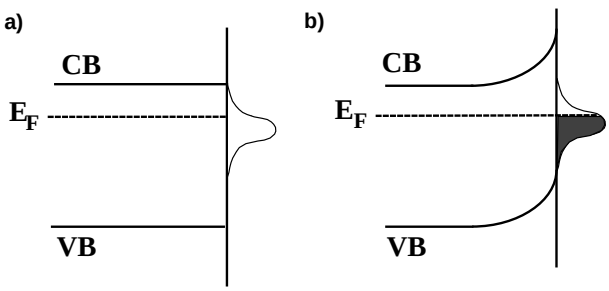

Figure 2. Idealized diagram relevant to chemical sensing of energy as a function of distance from the surface of an n-type semiconductor. (a) Semiconductor–gas interface (vertical line) before establishment of thermal equilibrium in the dark. Shown are the valence band (VB) and conduction band (CB) edges of the solid (separated by the band gap energy), the Fermi level, E_F, and a hypothetical distribution of surface states. (b) Establishment of thermal equilibrium in the dark. Electrons in the conduction band come from the bulk to fill the surface states up to the Fermi level (shaded portion of the hypothetical surface state distribution). This charge separation establishes an electric field in the near-surface region of the solid, represented by the bending of the band edges.

*Corresponding author.
**Present address: Department of Chemistry, Mercer University, 1400 Coleman Ave., Macon, GA 31207.

face: samples are typically etched before use with aqueous HCl and/or methanolic bromine solutions, followed by an ultrasonic treatment to facilitate removal of species that may be left on the surface by the etching procedure. It is noteworthy that the surface, despite its critical role in adduct formation, is poorly characterized under the experimental conditions generally employed for chemical sensing and may contain impurities (oxide phases, traces of water, etc.).

The electronic structure of these semiconductors is sketched in Figure 2 (*1*, *6*). Salient features are the valence band, comprising largely filled, closely spaced energy levels; and the conduction band, consisting of largely empty, closely spaced energy levels. The separation between the top of the valence band and bottom of the conduction band is the bandgap energy, E_g, and represents the threshold energy needed for absorption of light. Bandgap energies of CdS and CdSe are ca. 2.4 eV and 1.7 eV, respectively, corresponding to green and red light. In principle there are no electronic states within the bandgap, but at the surface of the solid, coordinative unsaturation and the presence of impurities may result in such intrabandgap surface states. Figure 2 shows a hypothetical distribution of surface states, with the shape indicating the largest density of these states in the middle of the distribution.

By analogy to water's role as a solvent for autoionization products (protons and hydroxide ions), the semiconductor can be regarded as a solvent for two kinds of oppositely charged carriers produced by autoionization: mobile conduction band electrons having concentration n, and mobile valence band holes having concentration p. The product ($n \times p$) is governed by an equilibrium constant, K, as is the case for autoionization in water. Both CdS and CdSe have chalcogen vacancies in the solid, which serve as electron donors (the solid must remain electrically neutral) and increase the concentration of mobile conduction-band electrons (*7*). Because $n > p$ in these materials, they are called "n-type," and the thermodynamic electrochemical potential in the solids, the Fermi level, lies near the conduction band edge, as shown in Figure 2.

At thermal equilibrium in the dark, the rate of production of electrons and holes by thermal excitation comes into balance with the rate of recombination processes. Photoexcitation above the bandgap energy perturbs the thermal equilibrium and creates additional electrons and holes, in a 1:1 ratio. The recombination of these particles across the bandgap can release energy as heat (quantized lattice vibrations, called phonons) or as light. In the latter case, the photons have roughly the bandgap energy of and represent the source of photoluminescence (PL) in CdS and CdSe, giving green and red light, respectively.

The photoexcitation can be continuous or pulsed. Most of the experiments described in this article are conducted with continuous excitation. Time-resolved experiments, however, afford the opportunity to monitor the decay of the excess electron-hole pairs in real time (*8*–*10*). A figure of merit in evaluating interfaces derived from semiconductors is the surface recombination velocity, S. This parameter has velocity units, typically cm/s, and reflects the rate at which minority carriers (holes in n-type materials) are consumed at the surface of the semiconductor. Large values on the order of 10^5 cm/s are common for unoptimized interfaces such as those used in our studies. With appropriate design considerations, including chemical treatments, values of S can be tuned over several orders of magnitude to enhance the performance of electro-optical devices.

Surface states can exert a profound effect on the recombination of excess carriers within the solid. It is energetically favorable for electrons from the bulk of the n-type solid to be trapped at the surface in the intraband gap states. Establishment of thermal equilibrium in the dark occurs when these states are filled with electrons up to the Fermi level, as shown in Figure 2. An important consequence of this process is that an electric field is now present in the near-surface region of the solid, reflecting the charge separation that has taken place. This field is represented by a bending of the band edges of the semiconductor, as illustrated in Figure 2. The near-surface zone that has been depleted of electrons (the majority charge carriers in n-type materials) is called the depletion region; and its thickness, the depletion width W, is on the order of 10^3 Å for typical CdS(e) carrier concentrations n of ca. 10^{16} cm^{-3}.

Adsorption Effects and Models for PL Response

Adsorption can in principle affect both the surface recombination velocity and the depletion width. Our studies have focused on adsorbates that appear to cause PL changes by altering the depletion width in a manner that reflects the Lewis acidity or basicity of the species. For example, adsorption of a Lewis basic molecule might cause electron density trapped in surface states to be shifted back into the semiconductor bulk, thereby reducing the depletion width. Conversely, an adsorbed Lewis acid might draw additional electron density into surface states from the semiconductor bulk, expanding the depletion width. Figure 3 compares these scenarios with the reference state corresponding to the absence of the adsorbate.

Treatment of the depletion width as a nonemissive zone or dead layer is a consequence of the electric field present therein: photogenerated electron-hole pairs can be separated by the field, with the direction of the field driving electrons to the bulk and holes to the surface in n-type materials; at the surface, the minority carriers are consumed through nonradiative surface recombination processes.

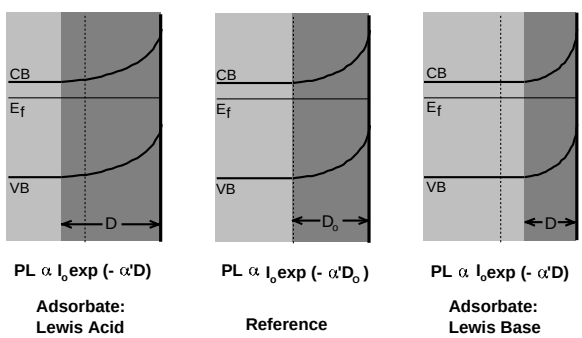

Figure 3. Chemical sensing based on modulation of the depletion width and PL intensity by surface adduct formation. The center figure represents the band bending present in the reference ambient, corresponding to a nonemissive zone or dead layer of thickness D_0 (compare Fig. 2b). Flanking this picture to the left and right are the thicker and thinner dead layers resulting from adsorption of Lewis acids and bases, respectively, from the ambient.

A simple model, the dead-layer model, treats the semiconductor as having a nonemissive zone on the order of the depletion width, and an emissive zone lying behind the dead layer in the bulk solid (*11*). The amount of light absorbed in this emissive zone is then proportional to the incident light intensity, I_o, and to $\exp(-\alpha D)$, where α is the absorptivity of the solid for the exciting light and D is the dead-layer thickness. The PL intensity will be proportional to $I_o\exp(-\alpha D)$ and reduced by a factor representing the reabsorption of emitted light as it travels through the crystal (self-absorption), $\exp(-\beta D)$, where β is the absorptivity of the solid for the emitted light. The absorptivity sum $(\alpha + \beta)$ is denoted α'.

For sensor purposes, the significant feature of the PL response is the ratio of the PL intensity in the reference ambient, PL_{ref}, and in the presence of the analyte of interest, PL_x, which eliminates the effects of geometric factors on the PL signal. The differential equations describing the generation, movement and recombination of charge carriers in the semiconductor lead to a so-called dead-layer model that expresses the PL change induced by the adsorbate quantitatively (eq 1):

$$PL_{ref}/PL_x = \exp(-\alpha'\Delta D) \qquad (1)$$

where ΔD is the difference in dead-layer thicknesses before and after adsorption, $(D_{ref} - D_x)$. Adsorption can also affect the surface recombination velocity. The dead-layer model assumes that adsorption either has no effect on S or that S remains large before and after adsorption ($S >> L/\tau$ and $S >> \alpha L^2/\tau$, where L and τ are the diffusion length and lifetime of the minority carrier in the solid, respectively) (*12*). More recently, a finite element numerical model has been used to quantify semiconductor PL and can be used to identify conditions under which accord with the dead-layer model can be anticipated (*13*).

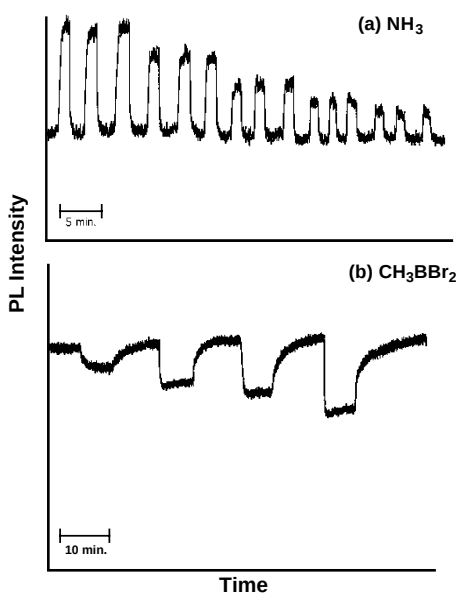

Figure 4. (a) Changes in PL intensity of n-CdSe resulting from alternating exposure to N_2 (initial response) and decreasing partial pressures of ammonia (ranging from 0.1 atm for the first trio of exposures to 0.001 atm at the end of the sequence). Adapted from ref *14a.* (b) Changes in PL intensity of n-CdSe resulting from alternating exposure to vacuum (initial response) and increasing pressures of CH_3BBr_2 (ranging from $\approx 3 \times 10^{-4}$ atm for the first exposure to $\approx 4 \times 10^{-2}$ atm, the last exposure). The maximum change in dead-layer thickness with exposure to the borane is 350 Å. In both experiments, PL was monitored at the PL band maximum, ≈720 nm. Adapted from ref *14b.*

If Lewis acidic and basic adsorbates are expected to alter the depletion width in opposite directions, then the PL signatures should move in opposite directions relative to a reference state. In the gas phase, both vacuum and nitrogen have been commonly used as reference states. Figure 4 demonstrates this "luminescent litmus test (*14*)". Ammonia, a Lewis base, is seen to enhance PL intensity reversibly relative to a nitrogen reference ambient for n-type materials. In contrast, methyldibromoborane, a Lewis acid, reversibly quenches PL intensity relative to a vacuum reference ambient. From the model presented, these effects should be reversed for p-type materials. Because, at low spectral resolution, the PL spectral distribution is unaffected by adduct formation, it is expedient to measure PL changes at a single wavelength, usually the band maximum. The concentration dependence of the PL effects will be discussed below, but the general observation is that the magnitude of the PL response increases with concentration until a saturation concentration is reached. The magnitude and speed of the PL response can be compared within a family of compounds to obtain a sense of the steric and electronic factors that contribute to the PL signatures.

When the compounds $(CH_3)BBr_2$, $(CH_3)_2BBr$, and $(C_2H_5)_3B$ were compared using the same CdSe sample, introduction of alkyl substituents was found to attenuate the quenching. This observation is consistent with reduction in the acidity of the borane by replacement of a halide substituent with an electron-donating alkyl substituent. But it is also consistent with less coverage of the surface by the more sterically demanding alkylated species. Because the PL method does not provide information about absolute coverage of the adsorbate, it has often proved difficult to account for trends in maximum PL response within a family of structurally and electronically related compounds. For ammonia and the boranes, a good fit to the dead-layer model was obtained for etched CdSe substrates. In addition, time-resolved PL data demonstrated that the PL decay traces obtained in nitrogen and in the presence of ammonia for the etched sample were indistinguishable, supporting the notion that the PL changes found in the continuous excitation experiments are driven principally by electric field changes rather than by changes in surface recombination velocity (*8*). The specific separation of these two factors-changes in electric field and surface recombination- is difficult in practice from transient PL measurements, since both factors depend on the relative magnitudes of the carrier lifetimes in the bulk and at the surface.

The concentration dependence of the PL response in experiments like those shown in Figure 4 can permit an estimate of the equilibrium binding constant K that is independent of surface coverage. The Langmuir adsorption isotherm model has been applied successfully to a number of CdS(e) substrates, including particulate as well as single crystal samples (*15*). Key assumptions of the Langmuir model are that all sites used for adsorption have identical binding enthalpies and that they do not interact with one another (*16*).

The quantitative form of the model may be derived from the equilibrium shown in eq. 2:

$$A + \sigma \rightleftharpoons A\cdot\sigma \qquad (2)$$

Here, σ is a surface site used for adsorption. A parameter θ represents the fractional surface coverage, with a value of zero representing the reference state and a value of one representing the saturated coverage, assumed to correspond to a monolayer. The forward rate is thus proportional to the ambient analyte concentration and the fraction of unoccupied sites, $(1-\theta)$; the reverse rate is proportional to the fraction of occupied sites θ. At equilibrium, the rates are equal, leading to the quantitative form for the adsorption isotherm model (eq 3):

$$\theta = KC/(1+KC) \quad \text{or} \quad 1/\theta = 1+(1/KC) \qquad (3)$$

Thus, a plot of θ vs. concentration will saturate at high concentration. A double reciprocal plot of $1/\theta$ vs. $1/C$ should be linear, with an intercept of unity and a slope whose reciprocal is the binding constant K. We have used both the fractional PL change and the fractional dead-layer thickness change resulting from adsorption to estimate θ. The latter typically gives better fits and represents θ as $\ln(PL_x/PL_{ref})/\ln(PL_{sat}/PL_{ref})$, where PL_{sat} is the saturated PL intensity found at high analyte concentration.

Film Transducers and Photochemistry

What of molecules that do not elicit a PL response? An example is dioxygen: relative to a nitrogen reference ambient, there is no PL intensity change from a CdSe substrate when dioxygen is introduced into the ambient, and the etched sample would be incapable of serving as a sensor. A strategy to embrace such analytes is to coat the solid with a thin film that can serve as a transducer: a chemical reaction of the analyte with the film can then alter the electronic structure of the underlying semiconductor, leading to a PL change.

This strategy has been successfully demonstrated using the cobalt salen complex shown below (*17*).

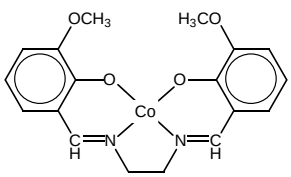

Calvin et al. demonstrated that this complex in the solid state will reversibly react with dioxygen to form a peroxo-bridged Co(III) dimer (*18*). A sample of CdSe can be coated with the Co complex simply by dissolving the complex in methylene chloride, placing a drop on the semiconductor, and allowing the solvent to evaporate.

When the coated solid is exposed to dioxygen, the PL intensity is quenched, as shown in Figure 5. The direction of the PL change is consistent with increased acidity upon oxidation of the Co complex comprising the film, as would be expected with the removal of electron density from the Co center. Interestingly, the fractional PL changes are not consistent with the dead-layer model. Larger fractional PL changes and thus larger values for ΔD are found with red light than with blue light, for example. This effect can be traced to photochemistry of the film, specifically to photoinduced dissociation of the dioxygen ligand. The oxygenated complex absorbs light at wavelengths shorter than ca. 620 nm. When 633-nm red light is used, the fractional PL change and value for ΔD are found to be independent of excitation intensity over a range of intensities exceeding an order of magnitude. In contrast, for the shorter wavelengths of light

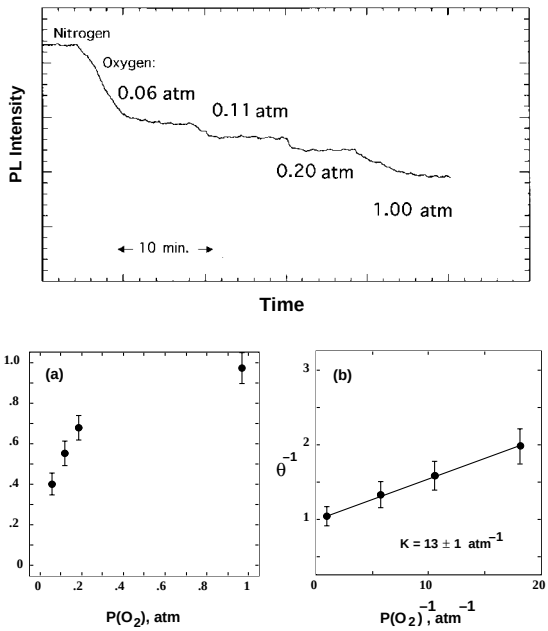

Figure 5. Upper panel: changes in the PL intensity of a Co(3-MeO-salen)-coated n-CdSe sample as a function of oxygen partial pressure; the reference level is nitrogen. Lower panels: left, fractional surface coverage θ vs. dioxygen partial pressure; right, double-reciprocal plot of the same data; the linearity of the plot (correlation coefficient of .99) represents a good fit to the Langmuir adsorption isotherm model, and the reciprocal of the slope yields an equilibrium constant K of 13 ± 1 atm^{-1}. Adapted from ref *17*.

that are absorbed (458 nm, for example), the fractional PL change and resulting value of ΔD increase as the excitation intensity is reduced, consistent with the notion that larger steady-state dioxygen concentrations can be produced in the film at lower incident intensities. This effect may be advantageous in sensor design in that sensing could be conducted by interrogating with long wavelength light where large PL changes occur, while the sensor sampling rate could be enhanced by occasional excitation at short wavelength, where the photochemistry of the film can be exploited to release the bound analyte, "resetting" the sensor.

The concentration dependence of the dioxygen response is shown in Figure 5, which indicates that the usable concentration range for the structure is ca. 0.01 atm to 1 atm. A good fit to the Langmuir adsorption isotherm model was obtained and the extracted binding constant, ca. 10–20 atm^{-1} for a variety of films, is in accord with values obtained by X-ray diffraction of freestanding, bulk oxygenated samples of the Co complex, which can be treated as solid solutions (*18*). This need not be the case, since, in principle, the environment at the semiconductor–film interface can be different from that within the bulk film, and a partitioning of the analyte between these two environments, quantified by a distribution coefficient, could occur. Since the PL response is expected to be most sensitive to the semiconductor–film environment, the binding constant obtained from this measurement could be different from the value of K characterizing the bulk film. For the case at hand, no such selectivity is seen, and the distribution coefficient would be approximately unity.

Sensor Structures and Considerations

Deployment of these sensor structures is illustrated by their introduction into a system designed to grow electronic materials by chemical vapor deposition (CVD), wherein precursor gases are decomposed on a heated substrate to yield solids (*1*). This technology permits the preparation of solids virtually an atomic layer at a time.

A simple design for PL-based sensing is to use a bifurcated optical fiber, sketched below.

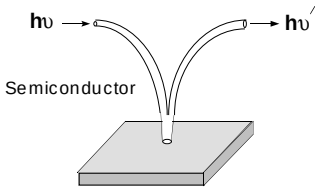

The semiconductor is excited through one leg of the fiber, and the emission, suitably filtered from the exciting light, is measured as it emerges from the other leg of the fiber. A chip of CdSe has been placed in the flow stream of a CVD apparatus and used to detect changes in the concentrations of ammonia, phosphine, and arsine in real time (*2*). The latter two gases are common precursors for the growth of semiconductors like GaP and GaAs. As expected, all three gases acted like Lewis bases, giving PL enhancements relative to the reference level, which is hydrogen carrier gas. Interestingly, the magnitude of the response was $NH_3 \sim PH_3 < AsH_3$, while all three compounds yielded similar binding constants of ca. 1000 atm^{-1}. The difference in PL response, which could be fit to the dead-layer model, might reflect a different binding mode for arsine and/or enhanced surface coverage. The similarity in binding constants could be interpreted in terms of countervailing trends: intrinsic basicity increases up this group in the periodic table, but binding to a moderately soft acidic surface site such as a Cd atom would be increasingly favored in passing down this group of compounds.

Although a laser and sophisticated detection instrumentation can be used for these experiments, an inexpensive alternative is to use an LED as a light source and two photocells, suitably filtered so that one measures scattered exciting light and one measures emitted light; this arrangement corrects PL intensity for variations in excitation intensity. A prototype of such a hybrid sensor has been constructed for placement directly into the CVD flow stream. All sensor components are derived from semiconductor structures and in principle lend themselves to incorporation onto a single chip in more advanced structures.

Practical Considerations

Use of these sensors hinges upon their ability to perform effectively under ambient manufacturing or environmental conditions. Key issues are selectivity, speed, sensitivity and ruggedness. The CVD chamber is an almost ideal testing ground from a selectivity standpoint because there are a limited number of species present. But in other environments, there may be a variety of species that can compete for adsorption sites and thus limit the usefulness of the semiconductor. The time needed for a response may be a critical factor and will reflect the adsorption and desorption kinetics of the substrate-analyte combination employed. We found, for example, that desorption of the group 15 hydrides described above from CdSe was extremely slow. While an increase in temperature could be used to enhance these rates, there is a trade-off with the signal-to-noise ratio: The quantum yield for PL declines with increasing temperature. Sensitivity plays a critical role in defining the concentration range over which an analyte-induced PL response can be observed. The range found for dioxygen detection with the coated CdSe sample, for example, would not be useful in environments where sensitivity to much lower trace concentrations would be desired. However, use of a coating with a far higher binding constant for dioxygen could permit such applications. Ruggedness remains a challenge for these sensors. For most of the studies conducted to date, sensor performance degrades with prolonged use, presumably reflecting competing irreversible surface chemistry.

While any given sensor element may have limited usefulness, it should be noted that a collection of such devices, each with a characteristic coupling of surface coordination chemistry and electro-optical properties, could provide adequate information for characterizing the composition of gaseous ambients comprising complex mixtures of gases.

Acknowledgments

We are grateful to the National Science Foundation and the donors of the Petroleum Research Fund, administered by the American Chemical Society, for generous support of this research.

Literature Cited

1. Ellis, A. B.; Geselbracht, M. J.; Johnson, B. J.; Lisensky, G. C.; Robinson, W. R. *Teaching General Chemistry: A Materials Science Companion*; ACS Books: Washington, DC, 1993; Wrighton, M. S. *J. Chem. Educ.* **1983,** *60*, 877.
2. Winder, E. J.; Moore, D. E.; Neu, D. R.; Ellis, A. B.; Geisz, J. F.; Kuech, T. F. *J. Crystal Growth* **1995,** *148*, 63; Lisensky, G. C.; Meyer, G. J.; Ellis, A. B. *Anal. Chem*. **1988,** *60*, 2531.
3. Lauerhaas, J. M.; Credo, G.; Heinrich, J.; Sailor, M. J. *J. Am. Chem. Soc.* **1992,** *114*, 1911.
4. Wells, A. F. *Structural Inorganic Chemistry*, 5th ed.; Clarendon: Oxford, 1984.
5. For a description of Miller indices, see West, A. R. *Solid State Chemistry and Its Applications*; Wiley: New York, 1992.
6. Ellis, A. B. *J. Chem. Educ.* **1983,** *60*, 332.
7. Hannay, N. B. *Semiconductors*; Reinhold: New York, 1959; Chapter 1.
8. Leung, L. K.; Meyer, G. J.; Lisensky, G. C.; Ellis, A. B. *J. Phys. Chem.* **1990,** *94*, 1214.
9. Evenor, M.; Gottesfeld, S.; Harzion, Z.; Huppert, D.; Feldberg, S.W. *J. Phys. Chem*. **1984,** *88*, 6213.
10. Lunt, S. R.; Ryba, G. N.; Santangelo, P. G.; Lewis, N. S. *J. Appl. Phys*. **1991,** *70*, 7449.
11. Hollingsworth, R. E.; Sites, J. R. *J. Appl. Phys*. **1982,** *53*, 5357.
12. Burk, A. A., Jr.; Johnson, P. B.; Hobson, W. S.; Ellis, A. B. *J. Appl. Phys*. **1986,** *59*, 1621.
13. Geisz, J. F.; Kuech, T. F.; Ellis, A. B. *J. Appl. Phys*. **1995,** *77*, 1233.
14. (a) Meyer, G. J.; Lisensky, G. C.; Ellis, A. B. *J Am. Chem. Soc.* **1988,** *110*, 4914; (b) Neu, D. R.; Olson, J. A.; Ellis, A. B. *J. Phys. Chem*. **1993,** *97*, 5713.
15. Chandler, R. R.; Coffer, J. L. *J. Phys. Chem*. **1991,** *95*, 4.
16. Atkins, P. W. *Physical Chemistry*, 5th ed.; W. H. Freeman: New York, 1994.
17. Moore, D. E.; Lisensky, G. C.; Ellis, A. B. *J. Am. Chem. Soc.* **1994,** *116*, 9487.
18. Calvin, M.; Barkelew, C. H. *J. Am. Chem. Soc.* **1946,** *68*, 2267; Hughes, E. W.; Wilmarth, W. K.; Calvin, M. *J. Am. Chem. Soc.* **1946,** *68*, 2273.